

Space-Energy Characteristics of Radiation Components Behind High-Energy Accelerator Shielding

D.V.Gorbatkov, V.P.Kryuchkov
 Institute for High Energy Physics
 Protvino, Moscow Region, Russia

Abstract

Space-energy characteristics of components of radiation fields (n, p, π, γ) behind high energy accelerators shielding were calculated by program complex ROZ/SADCO. The main regularities of radiation fields, formed in the concrete and iron shieldings, were investigated. The equilibrium of neutron spectrum in the concrete shielding and absence of it in the iron shielding were shown. The calculated numerous data of spatial and energy distributions of radiation components in the shielding and behind it can be used as a reference data.

1 INTRODUCTION

The data on characteristics of radiation fields behind shielding are required for solution of the most radiation and physical problem at high energy accelerators. Systematic calculational investigations of the space-energy distributions of radiation components behind one-dimensional radiation shielding of high energy hadron beam were carry out by using of program complex ROZ/SADCO [1,2]. The systematic error of the discrete-ordinates numerical method of transport equation solution, realized in code ROZ-6H [1], is less than 1%. The total accuracy of calculations is determined by errors of the constants from multi-group constant system SADCO [2] and amounts 30%.

2 GEOMETRY AND FUNCTIONALS

All investigations were carried out for one-dimensional homogeneous (concrete or iron) and heterogeneous (iron+concrete) geometries simulating real radiation shielding at accelerator. The spatial distributions of the following functionals were investigated: n_h - fluences of high energy neutrons ($E > 20\text{MeV}$), n_f - fast neutrons ($1\text{eV} < E < 20\text{MeV}$), n_{th} - thermal neutrons ($E < 1\text{eV}$), n_{ch} - fluence of all charged hadrons (protons and pions), n_γ - fluence of photons ($E < 20\text{MeV}$). The spectra of neutrons, protons, pions, photons as a function of a thickness of concrete and iron shielding and source particle energy were investigated too. The energy of source particle was varied in region $0.1 \div 100\text{ GeV}$.

3 SPATIAL DISTRIBUTION OF RADIATION

The spatial distributions of all components of radiation are presented in fig.1 ÷ 3. The main regularities of radiation fields, formed in the concrete and iron shieldings, as the following:

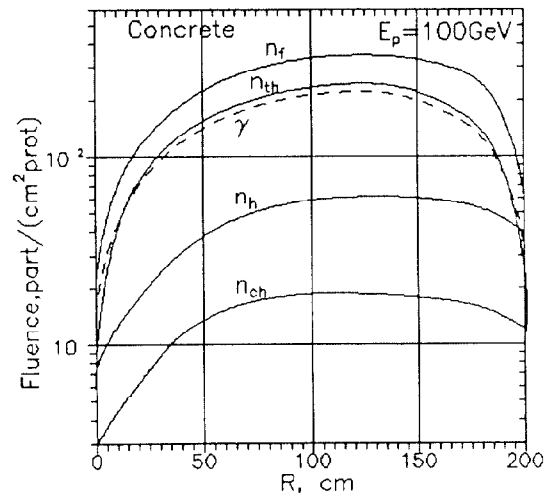


Figure 1: The spatial distribution of radiation components of fluence in concrete shielding for primary protons energy 100 GeV

- the spatial distribution very slowly depends on particle type if the particle energy is greater than 5 GeV;
- the attenuation of fluence of high energy hadrons (n, p, π) is exponential in over a length of all thickness of shielding, except the transition region. The index of exponent for neutrons is close to the index for charge particles;
- for concrete shielding the equilibrium between high energy components of hadrons and low energy components of neutrons is reached already in transition region;
- for iron shielding the equilibrium between high energy components and low energy components is absent. This fact was noticed in previous publications ([3,4]). The dependences of fluence of radiation components are presented in fig.4 for the side shielding and in table 1 for concrete, iron and heterogeneous (iron+concrete) shielding.

The very important fact follows from data of fig.4 and table 1 : relation between fluence of high energy hadrons and fluence of low energy neutrons behind concrete or heterogeneous (iron+concrete) shielding is independent on shielding thickness or energy of source hadrons. It can be presented as:

$$\Phi_n(E > 20\text{MeV})/\Phi_n(E < 20\text{MeV}) = 0,75 \pm 0,05.$$

The ratio of charged particle fluence to superfast neutron fluence depends on geometry and lies inside the interval $(0.15 \div 0.25)$.

Table 1: The components of radiation behind shielding (% of fluence).

1. Iron shielding, 100 cm					2. Iron shielding, 200 cm			
E, GeV	100	10	1	0,1	E, GeV	100	10	1
n_h	2,7	1,8	0,51	0,043	n_h	0,53	0,12	0,026
n_f	95,6	96,7	98,6	98,9	n_f	97,7	98,4	98,5
n_t	$2,4 \cdot 10^{-3}$	$2,8 \cdot 10^{-3}$	$5,9 \cdot 10^{-3}$	$1,4 \cdot 10^{-2}$	n_t	0,19	0,023	0,024
n_c	0,41	0,19	0,031	$1,6 \cdot 10^{-4}$	n_c	$6,4 \cdot 10^{-2}$	$9,4 \cdot 10^{-3}$	$1,3 \cdot 10^{-3}$
γ	1,2	1,38	0,9	1,1	γ	1,7	1,4	1,4

3. Concrete shielding, 200 cm				4. Side shielding (100 cm Fe + 100 cm concrete)			
E, GeV	100	10	1	E, GeV	100	10	1
n_h	27,3	27,1	27,1	n_h	9,9	9,6	5,4
n_f	36,3	36,2	35,6	n_f	13,4	12,2	6,9
n_t	7,5	8,0	8,1	n_t	6,2	5,9	5,2
n_c	8,4	6,7	6,1	n_c	1,0	0,96	0,39
γ	20,6	22,7	23,1	γ	69,5	71,3	82,0

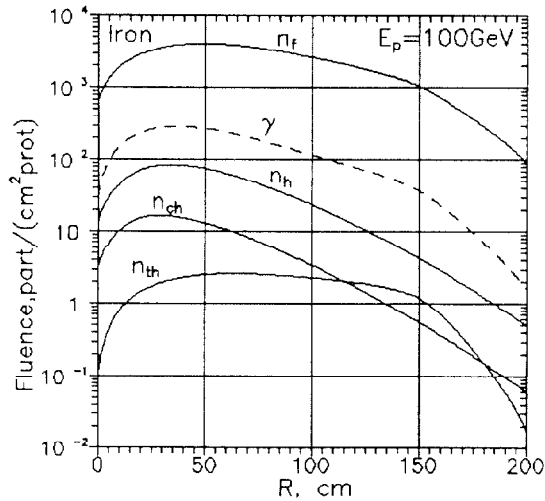


Figure 2: The same as in fig.1, but for iron shielding

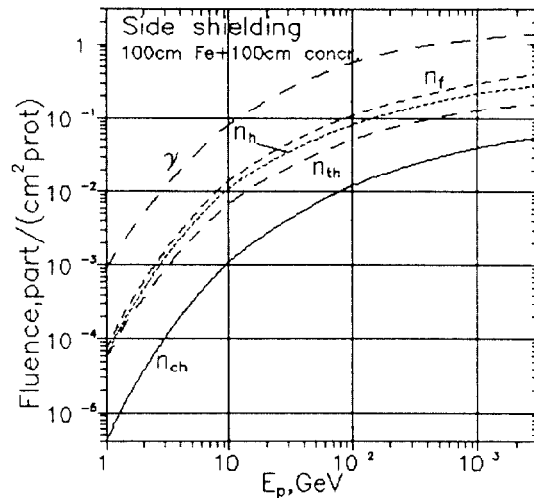


Figure 4: Energy dependence of radiation components of fluence for side shielding

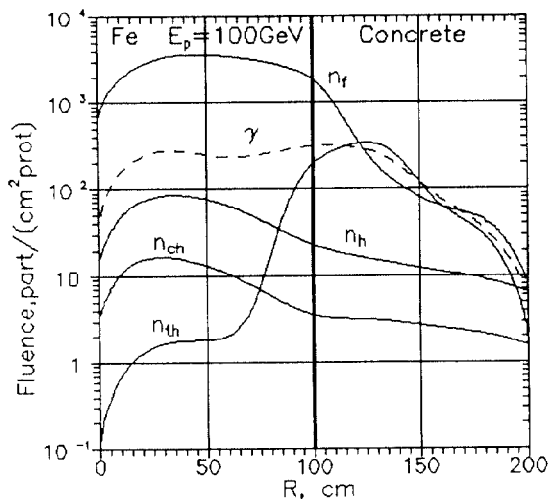


Figure 3: The same as in fig.1, but for heterogenous shielding

4 THE SPECTRA OF RADIATION

The proton and neutron spectra behind concrete in and side heterogeneous (iron+concrete) shielding are presented in fig.5,6. The data of fig. 5,6 show equilibrium of different components of radiation in the concrete shielding, indicated above. Shapes of neutron spectra for different thickness of shielding are similar and independent on energy and type of source particles. The neutron spectra behind iron in contrast one behind concrete have strong dependence on shielding thickness (fig.7). One can see the deformation of spectra with increasing of thickness. The calculated spectra of neutrons, protons, pions and photons behind iron shielding are presented in fig.8. One can see that :

- spectra of radiation very slowly depend on type of particle of the source;
- the maximum of proton spectra lies lower than maximum of neutron spectra;

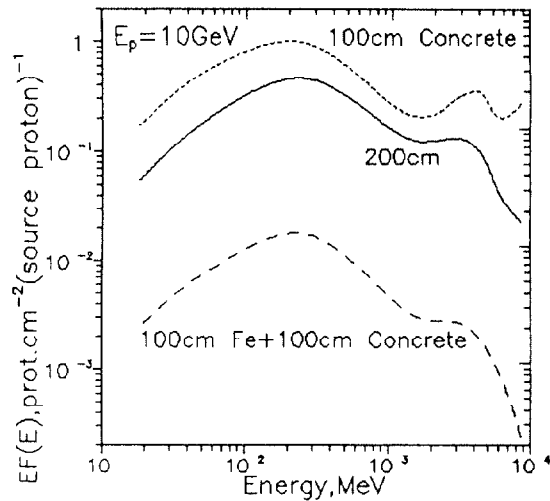


Figure 5: The protons spectra at various depth of concrete and heterogeneous(side) shielding for primary protons energy 10 GeV

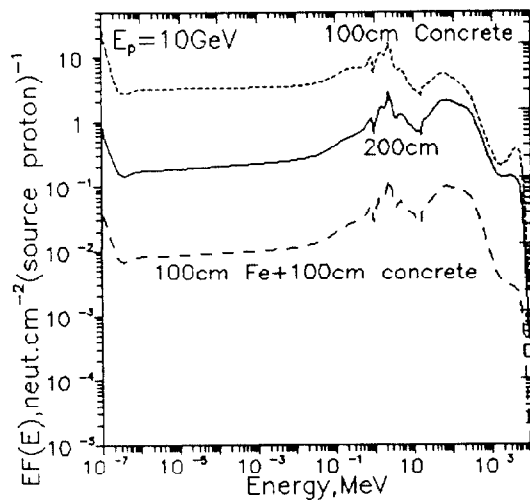


Figure 6: The same as in fig.5, but for neutron spectra

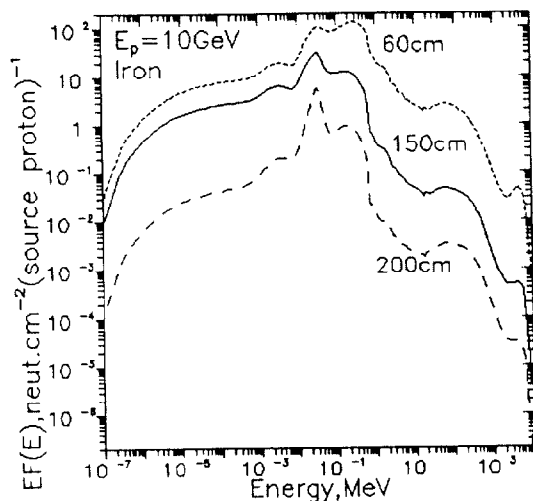


Figure 7: The same as in fig.6, but for iron shielding

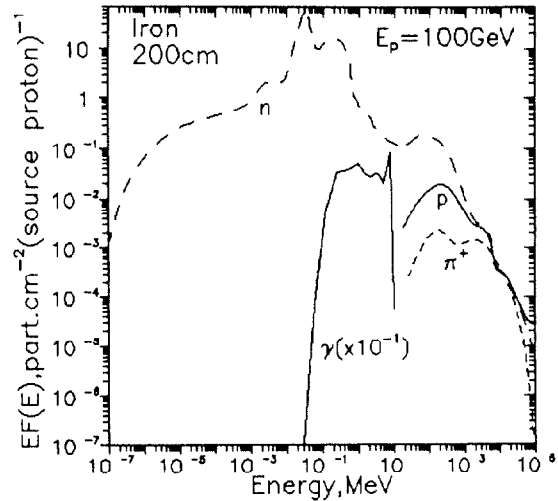


Figure 8: The radiation spectra behind 200 cm of iron shielding for primary protons energy 100 GeV

- the proton spectra as well as pion spectra has typical shape of a bell. There are two maximums for energy $E_0 > 10$ GeV. The maximum for pion lies lower than maximum for protons;
- the high-energy part of proton spectra nearly coincide with it of neutron spectra for energy of initial protons greater than 1 GeV.

5 CONCLUSION

The calculated numerous data of spatial and energy distributions of radiation components in the shielding and behind it can be used as a reference data. The existence of equilibrium between high energy and low energy components of radiation in concrete shielding and absence of it in iron shielding is shown. The relations between different component of radiation behind concrete and iron shielding are obtained.

6 REFERENCES

- [1] A.M. Voloschenko et al., Procs.Int.Top.Mtg.Adv.in Mathem., Comput. and Reactor Physics.- Pittsburg, USA, 1992.; A.M. Voloschenko, D.V. Gorbakov, V.P. Kryuchkov - Transaction of International Conference on "The Numerical Methods of Transport Equation Solving". - Moscow, 1992.
- [2] D.V. Gorbakov, V.P. Kryuchkov, Transaction of XIII Conference on Charged Particle Accelerators. - Dubna, 1992
- [3] V.P. Kryuchkov, Preprint IHEP 83-166.- Protvino, 1983.
- [4] K. Tesh, J.M. Zazula, Deutsches Elektronen-Synchrotron DESY 90-037, 1990.